buildings

MDPI

Article

Study on Horizontal Bearing Capacity of Pile Group Foundation Composed of Inclined and Straight Piles

Hongsheng Qiu [1], Heng Wang [1,*], Mo'men Ayasrah [2,*], Ziyu Zhou [3] and Bo Li [4]

[1] School of Transportation and Logistics Engineering, Wuhan University of Technology, Wuhan 430063, China
[2] Department of Civil Engineering, Faculty of Engineering, Al al-Bayt University, Mafraq 25113, Jordan
[3] Power China Corporation Guiyang Survey, Design and Research Institute Co., Ltd., Guiyang 550081, China
[4] China Railway Construction 11th Bureau, Boli, Wuhan 430061, China
* Correspondence: 305467@whut.edu.cn (H.W.); ayasrahmomen@aabu.edu.jo (M.A.)

Abstract: In all types of new arch bridge structures, the requirements of the foundation are becoming more and more strict. Under the action of horizontal thrust, the distribution of the internal forces of the pile group in which inclined piles participate in an arch foundation is complicated. In this regard, the horizontal forces of each pile in a pile group and the horizontal bearing performance of each pile in a pile group under the action of total thrust are investigated by establishing a pile group foundation model and a p-y curve difference equation. After an in-depth analysis of the simulation results, it is found that the load distribution calculated by the finite element method is very close to that calculated by the p-y curve method, both in terms of curve shape and numerical value, indicating that the pile top load distribution is close to the actual situation. In addition, the maximum shear force of each pile body occurs at the top of the pile, and the maximum bending moment occurs at the point 1/5 away from the top of the pile. Finally, the nonlinear analysis of the p-y curve method can be well applied to the calculation of bridge pile foundations.

Keywords: pile group foundation; horizontal thrust; finite element method; p-y curve method

check for updates

Citation: Qiu, H.; Wang, H.; Ayasrah, M.; Zhou, Z.; Li, B. Study on Horizontal Bearing Capacity of Pile Group Foundation Composed of Inclined and Straight Piles. *Buildings* **2023**, *13*, 690. https://doi.org/10.3390/buildings13030690

Academic Editor: Alberto Maria Avossa

Received: 6 February 2023
Revised: 28 February 2023
Accepted: 3 March 2023
Published: 6 March 2023

Copyright: © 2023 by the authors. Licensee MDPI, Basel, Switzerland. This article is an open access article distributed under the terms and conditions of the Creative Commons Attribution (CC BY) license (https://creativecommons.org/licenses/by/4.0/).

1. Introduction

As urban infrastructure continues to improve, urban municipal bridges are moving toward new types that are lightweight and beautiful. The rise of a large number of special-shaped arch bridges has put forward new requirements for pile group foundations for bridges. Under the implementation of the upper load, the special-shaped arch bridge needs to rely on a pier and foundation to resist the larger horizontal thrust in order to avoid local defects or even damage during the service period, so it is necessary to pay attention to the research on the horizontal bearing performance of pile group foundations. Under horizontal thrust, the internal force distribution of the pile base is complicated, and there are many factors that affect the load capacity of the pile. In order to avoid the excessive displacement of the pile group foundation affecting the arch circle of the special-shaped arch bridge and the excessive additional stress resulting in structural damage during service, it is particularly important to ensure the horizontal stability of the pile group [1].

It Is well acknowledged that the responses of the pile under combined loads may be notably different from the responses of the pile under pure axial or horizontal loads owing to the axial and lateral loads interaction [2,3]. In addition to these studies, numerous studies have been conducted to examine how piles respond to inclining loads or combination loads [4–9]. In addition, compared with a dry soil and saturated soil condition, the horizontal displacement and bending moment of the pile in an unsaturated soil condition are smaller [10]. In general, the lateral displacement of supporting piles under horizontal loads is more than tens of millimeters [11], and soil mass can yield and produce plastic deformation [12,13].

Elastic theory alone does not meet the requirements of practical engineering. As a result, many domestic and international scholars have adopted the p-y curve approach to describe the nonlinearity of pile–soil contacts in various soil layers. Therefore, in order to assess the impact of the vertical loads on the lateral behavior of the piles, it is required to examine the influence of the vertical loads on the p-y curves of the laterally loaded piles [14]. Moreover, a series of studies [15–22] have been carried out, and some scholars have applied the p-y curve method to inclined pile foundations [23,24].

With that in mind, the interaction between the vertical and lateral loads is not taken into account by the conventional approach for analysis of the laterally loaded piles based on subgrade reaction methods. Therefore, based on the bearing characteristics of the arch bridge pile group, in this paper, a 3D finite element model is established to analyze the bearing capacity of the pile group in the horizontal direction and verified the feasibility of the model according to the field experimental data. In addition, the rationality of the p-y curve method for the calculation of bridge pile foundation under the basic combined load transmitted by the superstructure was also investigated.

2. Engineering Background

2.1. Project Overview

The proposed construction site of the Jindao Bridge is located in Jinwan District, Zhuhai City. It is a special-shaped arch bridge spanning the main flood drainage channel in the second phase of the municipal supporting project, as shown in Figure 1. The bridge starts at KC0+132.00 and ends at KC0+232.00. The span of the bridge is 100 m. The design grade is a bidirectional, six-lane urban main road, and the bridge layout is shown in Figure 2.



Figure 1. The rendering of golden island bridge.

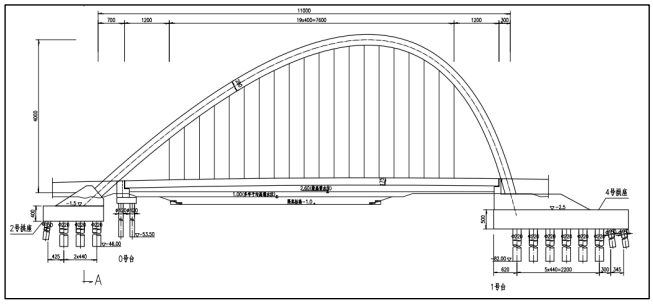
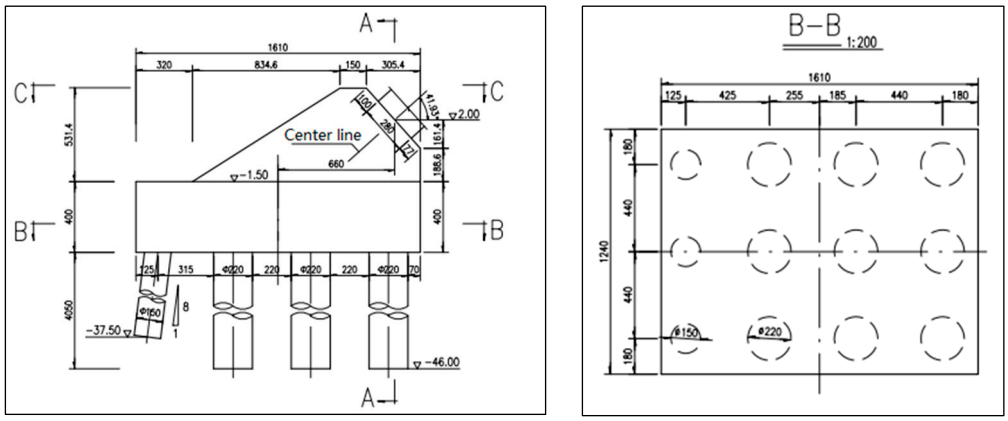


Figure 2. The elevation of arch rib No. 2.

2.2. Pile Foundation Layout Scheme

The arch seat and bearing pile cap are made of C40 concrete. The cap dimension of No. 2 arch seat is 12.4 m × 16.1 m and its thickness is 4.0 m. Nine C30 bored cast in situ

piles with a diameter of 2.2 m and three inclined piles with a diameter of 1.5 m are used as the modeling object in this paper. The Arch structure diagram is shown in Figure 3.



(**a**) (**b**)

Figure 3. Structure diagram of arch seat: (**a**) elevation plan; (**b**) plan of piles cap foundation.

2.3. Engineering Geology Overview

The drilling revealed that the rock and soil layers are divided into artificial fill (Q^{4ml}), Quaternary Marine and Continental Inter Sedimentary Layer (Q^{4mc}), residual layer (Q^{el}), Yanshanian III ($\gamma^{52(3)}$) granite regolith, and Devonian (D) sandstone regolith. The soil layers from top to bottom are: (1) Artificial soil filling, with a layer thickness of 0.50~4.50 m, and an average thickness of 2.80 m. (2) The sea–land cross-sedimentary layer (Q^{4mc}): silty soil—grayish-brown, wet, soft plastic, mainly composed of clay particles, and a small amount of fine sand in some parts, with a layer thickness of 17.80~38.60 m, and an average thickness of 26.23 m; silty clay—partially exposed as clay, with an exposed layer thickness of 0.50~8.50 m, and an average thickness of 3.51 m; coarse sand—the layer is mainly coarse sand, with exposure as medium sand with a thickness of 0.50~7.12 m, and an average thickness of 2.53 m. (3) Residual layer (Q^{el}): This layer is mainly composed of sandy clay, with an exposed layer thickness of 1.20~17.30 m, and an average thickness of 7.68 m. (4) Yanshanian third-stage granite ($\gamma^{52(3)}$): strongly weathered granite, yellowish-brown, grayish-brown, grayish-white, very broken rock mass, fissure development, core is half rock and half earth, with an exposed layer thickness of 5.30~41.60 m, and an average thickness of 17.04 m. The soil properties are shown in Figure 4.

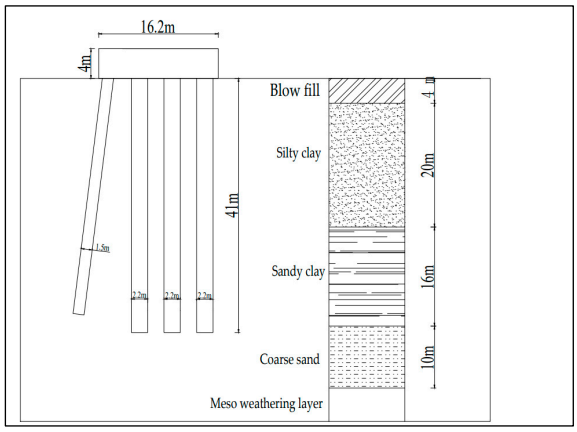


Figure 4. Soil profile and typical section in this study.

2.4. Stage of Construction and Field Mesurements

Horizontal Static Load Test of Single Pile

It is fundamental to note that the vertical and inclined piles are named as (2-8#) and (2-X2#), respectively. In addition, the vertical pile was tested in the arch foundation "2-8#", where "2" represents the arch seat label, "8#" represents the pile tested, and "2-8#" means a test vertical pile of the second arch foundation. The inclined pile to be tested is named "2-X2#", where the first "2" also represents the arch seat label, "X" is the letter added to distinguish the vertical pile, "2#" represents the inclined pile to be tested, and "2-X2#" means a test inclined pile of the second arch seat foundation. In this test, a 2-8# vertical pile and a 2-X2# inclined pile were tested under horizontal static load using the slow maintenance load method, in accordance with the Technical Specifications for Testing Building Foundation Piles (JGJ106-2014) [25]. The loading test adopts 10-stage loading, and the initial loading value is 2 fold the design load, while the unload at each level was twice the design loading, and it was the same amount step by step. The test stages are as follows:

1. The pile top settlement is observed in 5, 15, 30, 45, and 60 min within the first hour of application, and then every 30 min thereafter; if the settlement is less than 0.1 mm within one hour and the value of two observations is still less than 0.1 mm, the settlement is relatively stable. When the settlement is relatively stable, the next level of load can be applied.

2. During unloading, each level of load was maintained for 1 h, and the piles were observed according to 15, 30, and 60 min, respectively. When unloading to 0, the amount of participating sedimentation shall be read, and the duration shall be no less than 3 h. The measurement time shall be 15 min and 30 min, and then the measurement shall be carried out every 30 min.

3. Stop loading when the pile body is damaged or the horizontal displacement exceeds 30–40 mm, and the horizontal displacement exceeds one of the design requirements.

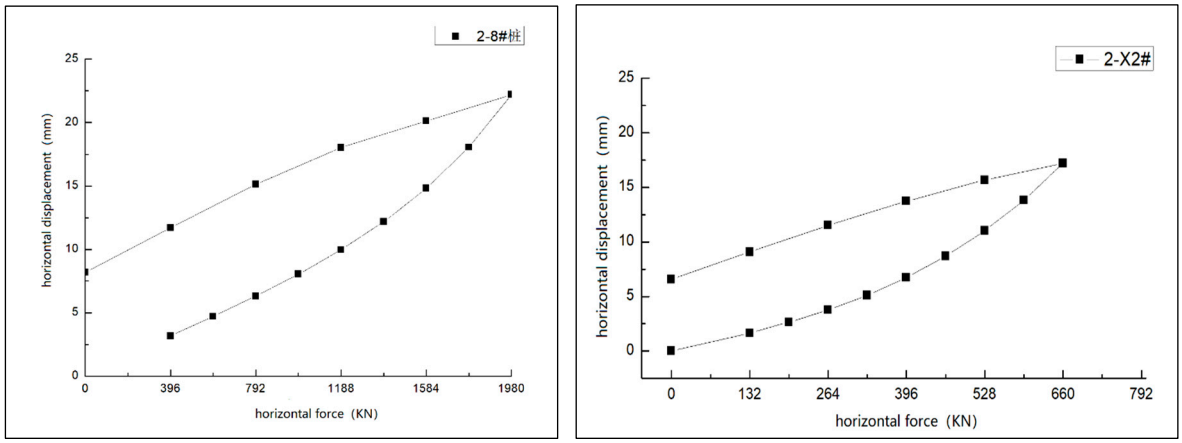
The test data are shown in Tables 1 and 2, respectively. In addition, the test data are plotted as the relation curve of horizontal force-horizontal displacement ($H_0 - x_0$) and horizontal force–displacement gradient ($H_0 - \Delta x_0 / \Delta H$), as shown in Figures 5 and 6, respectively.

Table 1. Settlement result table of No. 2-8# pile under graded loading.

Serial Number	Load (kN)	Time Consumed (min)		Settlement (mm)	
		Each Level	Accumulation	Each Level	Accumulation
0	0	0	0	0	0
1	396	150	150	3.17	3.17
2	594	150	300	1.54	4.71
3	792	120	420	1.61	6.32
4	990	120	540	1.72	8.04
5	1188	120	660	1.93	9.97
6	1386	120	780	2.21	12.18
7	1584	120	900	2.63	14.81
8	1782	120	1020	3.24	18.05
9	1980	120	1140	4.14	22.19
10	1584	120	1260	−2.07	20.12
11	1188	60	1320	−2.09	18.03
12	792	60	1380	−2.89	15.14
13	396	60	1440	−3.43	11.71
14	0	60	1500	−3.52	8.19
Maximum settlement value: 22.19 mm; maximum rebound value: 8.19 mm Rebound rate: 36.91%					

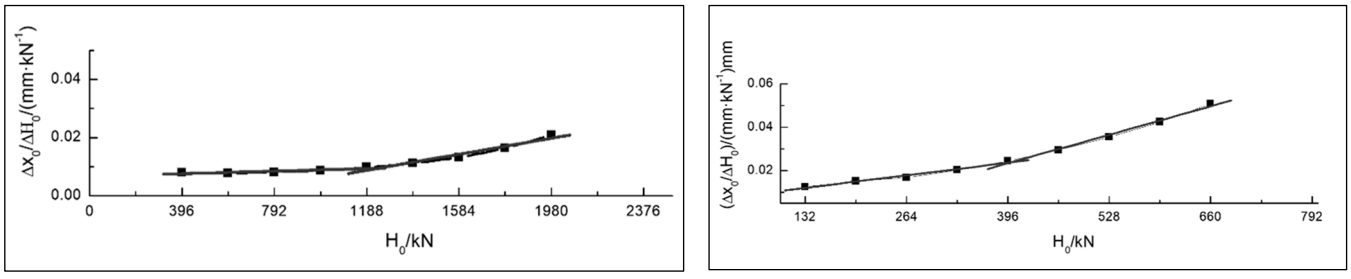
Table 2. Settlement result table of No. 2-X2# pile under graded loading.

Serial Number	Load (kN)	Time Consumed (min)		Settlement (mm)	
		Each Level	Accumulation	Each Level	Accumulation
0	0	0	0	0	0.00
1	132	180	180	1.66	1.66
2	198	150	330	1.00	2.66
3	264	150	480	1.11	3.78
4	330	120	600	1.34	5.12
5	396	120	720	1.62	6.74
6	462	120	840	1.95	8.69
7	528	120	960	2.34	11.03
8	594	120	1080	2.80	13.83
9	660	120	1200	3.35	17.18
10	528	120	1320	−1.53	15.66
11	396	60	1380	−1.93	13.73
12	264	60	1440	−2.22	11.51
13	132	60	1500	−2.43	9.08
14	0	60	1560	−2.50	6.58
Maximum settlement value: 17.18 mm; Maximum rebound value: 6.58 mm Rebound rate: 37.64%					



(**a**) (**b**)

Figure 5. Horizontal force–displacement $(H_0 - x_0)$ curve of: (**a**) 2-8# pile; (**b**) 2-X2# pile.



(**a**) (**b**)

Figure 6. Horizontal force–displacement gradient $(H_0 - \Delta x_0/\Delta H)$ curve of: (**a**) 2-8# pile; (**b**) 2-X2# pile.

The horizontal thrust of the 2–8 pile is stable under a test load of 1980 kN, the maximum horizontal displacement is 22.19 mm, the curve of $(H_0 - \Delta x_0/\Delta H_0)$ is good, there is no obvious inflection point, and the horizontal ultimate bearing capacity of single pile is $H_0 \not< 1980kN$.

Under a test load of 660 kN, the horizontal thrust of 2-X2# pile is stable, the maximum displacement is 17.18 mm, the curve of $(H_0 - \Delta x_0/\Delta H_0)$ is good, there is no steep section, no obvious inflection point, and the horizontal ultimate bearing capacity of the single inclined pile is $H_0 \not< 600kN$, which meets the design requirements.

3. P-Y Curve Model Calculation Theory

3.1. Calculation of Horizontal Bearing Capacity of Vertical Single Pile by the P-Y Curve Method

Under the implementation of load, the pile deflection differential equation is established:

$$EI\frac{d^4y}{dz^4} = p(y,z) - kby \tag{1}$$

where EI is the flexural stiffness, y is the horizontal displacement of the pile, b is the diameter of the pile, k is the secant modulus of p-y curve at z depth, and $p(y,z)$ is the modulus of subgrade reaction.

Use difference instead of differential, divide the front and back piles into n parts, a total of n+1 nodes. To facilitate the calculation of nodes at both ends, four virtual nodes are added as shown in Figure 7:

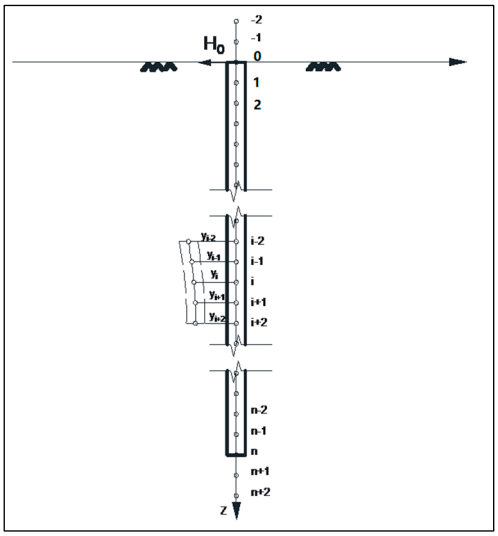


Figure 7. The single pile node division diagram.

From the fourth-order central difference formula:

$$y_{i-2} - 4y_{i-1} + \left(6 + \frac{k_i bh^4}{E_f I_f}\right)y_i - 4y_{i+1} + y_{i+2} = \frac{h^4}{E_f I_f}q_i \tag{2}$$

n+1 nodes can list n+1 equations, listing pile end boundary conditions:

$$\begin{cases} y_{-2} - 2y_{-1} + 2y_1 - y_2 = 0 \\ y_{-1} - 2y_0 + y_1 = 0 \\ y_{n-2} - 2y_{n-1} + 2y_{n+1} - y_{n+2} = 0 \\ y_{n-1} - 2y_n + y_{n+1} = 0 \end{cases} \tag{3}$$

MATLAB is used to calculate nonlinear equations iteratively. The calculation process is as follows:

(1) To define parameters, referring to the «Technical Specification for Building Pile Foundation» (JGJ94-2008) [26], firstly define $k^{(0)} = m(i \cdot h - H)$; m is taken as $2 \times 10^6\ kN/m^4$ according to field experience, and h is the distance between two nodes.

(2) According to assumption $k_i^{(0)}$, a set of solutions $y^{(1)}$ is obtained, and the obtained solution $y^{(1)}$ is substituted into the p-y curve to obtain $p^{(1)}$ in the set of solutions. Let $k_i^{(1)} = p_i^{(1)} \Big/ y_i^{(1)}$.

(3) Substitute $k^{(1)}$ again to solve the next set of displacement vectors $y^{(2)}$ until a set of $k^{(n)}$ is obtained so that the infinite norm of the vector of two displacement solutions is less than 1 mm, that is, $||y^{(n)} - y^{(n-1)}||_\infty =< 0.001m$. Iteration converges and the cycle ends.

(4) According to the obtained vector $y^{(n)}$, multiplied by the corresponding matrix, the pile angle vector θ, the node shear vector Q and the node bending moment vector M are obtained.

3.2. Calculation of Horizontal Bearing Capacity of the Inclined Pile by the P-Y Curve Method

It is worth mentioning here that when the horizontal force direction is opposite to the inclined direction of the pile, and it is referred to as a negatively inclined pile, while when the horizontal force direction is equivalent to the inclined direction of the pile, it is referred to as a positively inclined pile. However, under horizontal load, the load of a negatively inclined pile can be decomposed into a normal load and an axial load, assuming that the axial force is in equilibrium. In order to simplify calculation, the differential equation of the deflection of the inclined pile is obtained when the side friction of the pile is ignored.

$$EI\frac{d^4y}{dz^4} + N\frac{d^2y}{dz^2} - p(y,z) = 0 \tag{4}$$

The fourth-order central difference is expanded as follows:

$$y_{i-2} + \left(h^2\frac{N}{E_fI_f} - 4\right)y_{i-1} + \left(6 + \frac{k_ibh^4}{E_fI_f} - 2h^2\frac{N}{EI}\right)y_i + \left(h^2\frac{N}{EI} - 4\right)y_{i+1} + y_{i+2} = \frac{h^4}{E_fI_f}q_i \tag{5}$$

Meyerhof and Yalcin [4] analyzed the distribution of the ultimate soil resistance of the inclined pile through field tests and showed that the ultimate soil resistance of the inclined pile increased linearly with depth, from on the surface to the maximum value. This method can be used to analyze the bearing performance of the inclined pile under horizontal load.

4. Establishment and Verification of Finite Element Numerical Model

4.1. Constitutive Model and Geometric Model Establishment of Soil

The main content of this paper is the bearing characteristics of pile group thrust foundations under horizontal force. It is well acknowledged that the material properties of soil are complex, and the mechanical properties of soil are not the same even for the same type of soil [27]. When analyzing problems, a relatively reasonable constitutive model is often adopted according to the actual engineering situation. The model to be established in this paper should consider loading and un-loading according to the field detection test of actual engineering. It is more reasonable to adopt the Modified Mohr–Coulomb model, which is a combination of nonlinear and plastic models, as the constitutive model of native soil body, which can well describe the resilience of soil in unloading.

When the finite element method is used to analyze pile–soil contact, the dimension of soil in the model is very important to the calculation of pile–soil interaction. If the calculation range of soil is too small, the bearing capacity of foundation soil cannot be truly reflected, and the horizontal resistance of soil to piles will be underestimated. However, too close boundary constraints will have an effect on the pile foundation, causing the simulation results to be distorted. If the soil mass calculation range is too large, the grid element will be wasted, and the memory and time required for calculation will be too large. Mengou and Xiaoping [28] provides a basis for determining the calculation range of soil around the pile in the finite element analysis of a pile-raft foundation, and the calculation results showed that the soil mass around the pile with twice the pile length can meet the accuracy requirements with a small number of grids. Moreover, three-dimensional models

of an arch bridge cap and pile group of the same size are established according to the construction drawings, as shown in Figure 8.

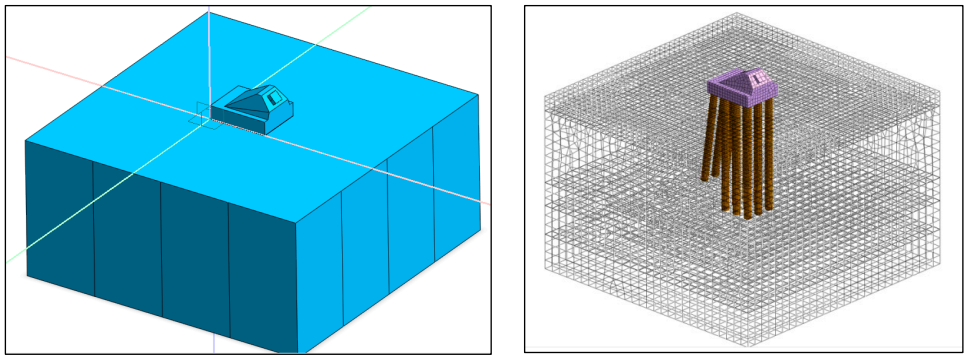


Figure 8. Geometry model and 3D finite element mesh.

To sum up, in this paper, twice the pile length is taken as the dimension of foundation soil in this model, and a soil model with length × width × height of 80 m × 80 m × 60 m, respectively, is established. In addition, a roller was assumed on the side of the model to allow movement in the vertical direction, and a pin was placed at the end of the lower soil to prohibit any movement in any direction. A relatively fine mesh was utilized close to the piles due to the increase in wide shear strains, whereas a coarser mesh was used further outside of these zones. On the other hand, a linear elastic model was used to simulate the piles, pile caps.

It is worth mentioning that in most cases, E_{oed} is the value of the soil compression modulus and $E_{50} = 2E_{oed}$ for soft clay and $E_{50} = E_{oed}$ for silty and sandy soil. $E_{un} = 4$ fold E_{50} for soft clay and 3 fold E_{50} for sandy soil [29–31]. In addition, the coefficient of lateral earth pressure (k_0) at rest is determined using the equation suggested by Jacky (1944) [32].

$$k_0 = 1 - \sin \varnothing \quad (6)$$

Therefore, soil material and structural properties are shown in Tables 3 and 4, respectively.

Table 3. Soil layer engineering parameters.

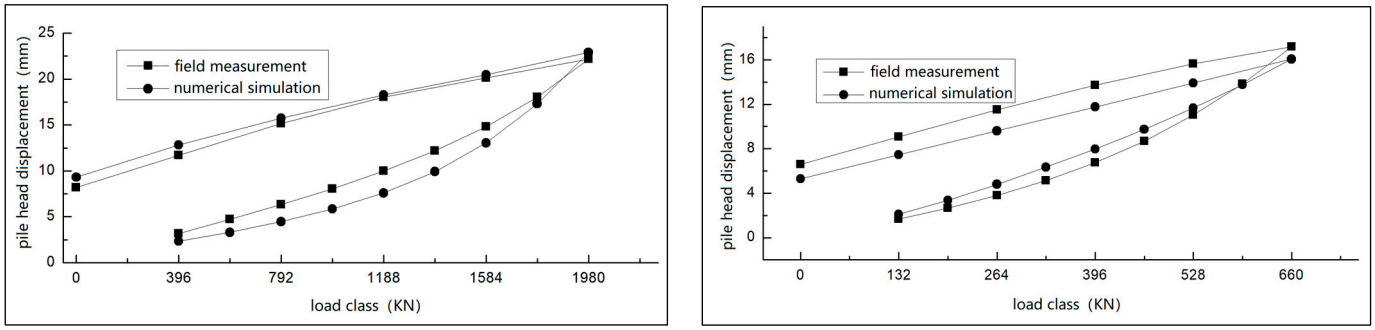
Parameter \ Soil Layers	Blow Fill	Silty Clay	Sandy Clay	Coarse Sand	Meso Weathering
Thick (m)	4	20	16	10	-
Unit weight (kN/m^3)	20.3	16.5	18.3	20.5	-
Friction angle (0)	23.6	18.0	18.0	24.3	24.7
Cohesion (kPa)	10	15.2	21.2	22.7	23.2
Lateral earth pressure coefficient (-)	0.31	0.31	0.28	0.3	0.3
Poisson's ratio (-)	0.31	0.34	0.28	0.30	0.30
Triaxial loading stiffness E_{50} (mPa)	8.04	2.23	2.23	11.01	5.42
Oedometer loading stiffness E_{oed} (mPa)	8.04	2.23	4.04	11.01	5.42
Triaxial unloading stiffness E_{ur} (mPa)	24.12	6.69	12.12	33.03	16.26

Table 4. Structural properties adopted in the numerical analysis.

Parameters	Pile	Pile Cap
Elastic Modulus (mPa)	3×10^5	3.25×10^7
Unit Weight (kN/m^3)	23.5	25
Poisson's Ratio	0.2	0.2

4.2. Verification of the Numerical Model

The field horizontal bearing tests were verified by the numerical model by using the same loading sequence as in the field test. The results are shown in Figure 9.



(**a**) (**b**)

Figure 9. The load–displacement curve ($H_0 - x_0$) of: (**a**) Pile 2-8#; (**b**) Pile 2-X2#.

The results show that under the same loading conditions, the shape and value of the displacement load curve are very close to the measured results, indicating that the selection of soil parameters is close to the actual situation, and the pile–soil contact can better reflect the actual situation. The numerical model is basically consistent with the actual situation and can be used for subsequent analysis.

5. Study on Horizontal Bearing Capacity of a Single Pile in a Group Consisting of an Inclined Pile and a Non-Inclined Pile

Based on the pile group foundation model and the p-y curve method, the horizontal force of each pile in the pile group is analyzed, and the horizontal bearing performance of each pile in the pile group under the action of the total thrust is determined.

5.1. The Internal Force of Each Pile under Horizontal Load

According to the bridge model established by Midas Civil software, as shown in Figure 10, the design value of the load transferred by the superstructure under the condition of basic combination is determined.

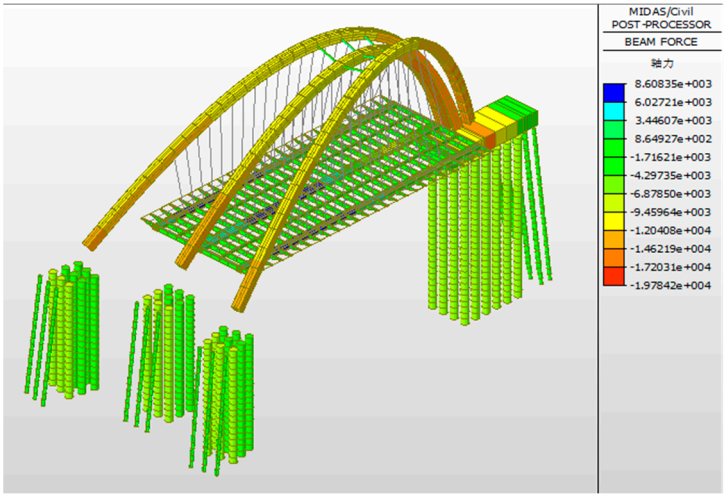


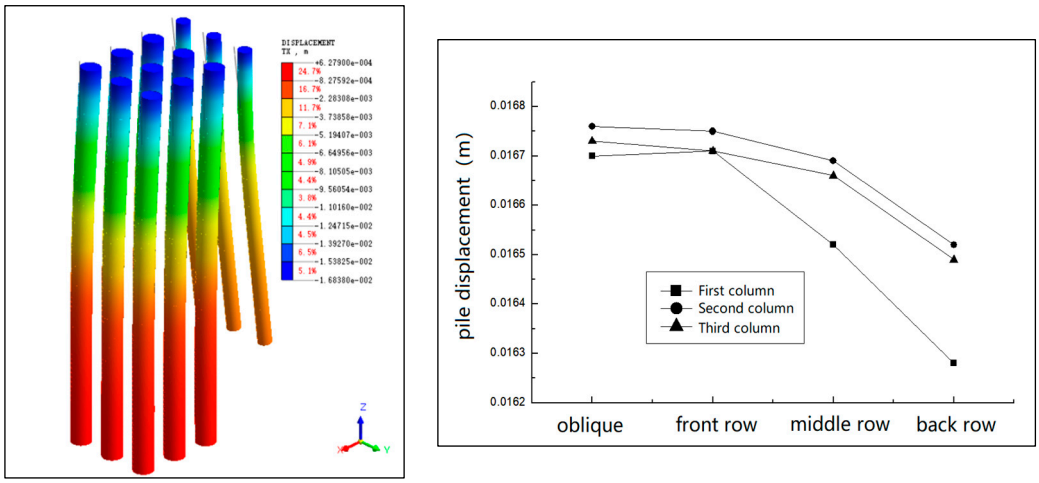
Figure 10. Axial diagram of JinDao bridge.

5.1.1. The Internal Force of Each Pile in Pile Group

Referring to the Midas Civil bridge design model and the Midas GTS NX finite element model of the pile group, the internal forces and dispositions of the pile top under the design load after completion of the bridge are compared, so as to analyze the distribution of the internal forces of the pile top in the horizontal thrust foundation.

(1) Pile Displacement

Under the action of horizontal thrust, the displacement behavior of the pile group foundation is shown in Figure 11.



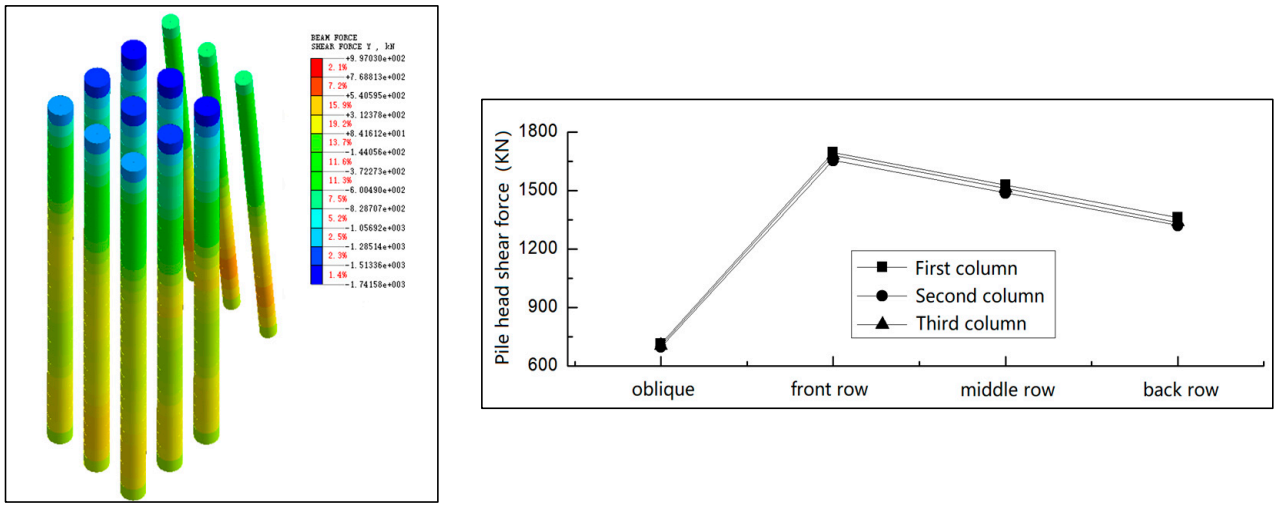
(**a**) (**b**)

Figure 11. Piles group displacement behavior of the piles top.

As can be seen from Figure 11, under the horizontal thrust of the design load, the overall displacement trend of each pile is approximately the same, and the maximum displacement of the pile top is approximately 16.7 mm. It is minimal at the pile end all the time: It reduces with depth. The actual maximum displacement difference between piles is only 0.3 mm, indicating that the top displacement of the three columns of piles is very close. Therefore, in the follow-up study, the average value of the three columns of piles as the research object.

(2) Shear Force of the Pile

Under the action of horizontal thrust, the shear force of pile group foundation is shown in Figure 12.



(**a**) (**b**)

Figure 12. Diagram of maximum shear force on top of each pile.

It can be seen from Figure 12 that under the effect of horizontal thrust under the design load, the shear diagram of each pile has a similar variation trend along pile depth. The maximum value of the shear diagram is at the top of the pile, and with the increase in depth, the shear diagram rapidly decreases near the top of the pile, and negative shear

occurs at a certain depth, and decreases to zero at the bottom of the pile. Similarly, the maximum displacement of piles in each column is similar, so the average value of shear forces in the three columns is taken as the follow-up study.

(3) Bending Moment of the Pile

By integrating shear along the pile length, the bending moment of each pile body of an inclined and straight pile group foundation is obtained, as shown in Figure 13, and the maximum bending moment of each pile body is shown in Figure 14.

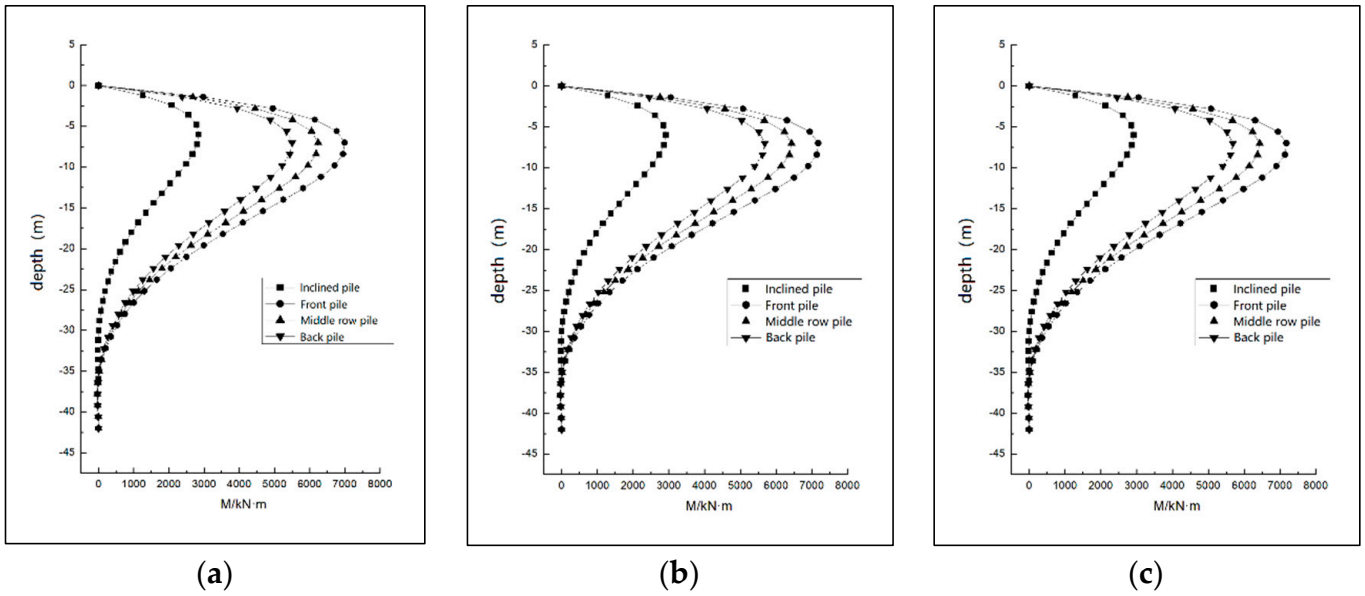


Figure 13. Pile bending moment behavior: (**a**) first column; (**b**) second column; (**c**) third column.

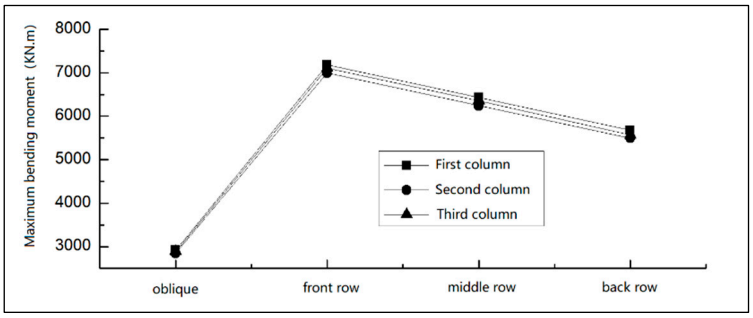


Figure 14. Maximum bending moment diagram of each pile body.

It can be seen from Figures 13 and 14 that under the effect of horizontal thrust of the design load, the bending moment diagrams of each pile have a similar variation trend along pile depth. The bending moment of the pile body first increases and then decreases, and the maximum bending moment is 5–10 m under the pile head (shear at 0).

5.1.2. Pile Top Internal Force Distribution

Under the design load, pile column shares the thrust force transmitted from the arch ring with little difference between them. When discussing the distribution of the pile top internal force, the average value of the pile top internal force for the three columns is taken. The shear force of the pile top along the bridge is shown in Figure 15.

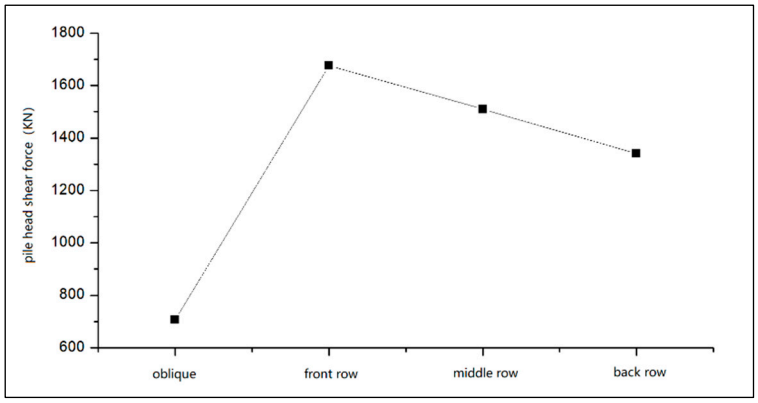


Figure 15. Shear force diagram of pile top under design load.

Under the action of a basic capacity combination, the ratio between the mean value of the pile top shear and the sum of the pile top shear in each row can be regarded as the proportion of the pile top shear undertaken by each row, which can be regarded as the proportional distribution of shear in each row along the bridge. The distribution proportion is as follows: 13.50% for the inclined pile, 32.04% for the front row pile, 28.85% for the middle row pile, and 25.61% for the back row pile. The calculated results of horizontal displacement were compared with the results calculated by p-y curve theory and the field experiments as shown in Figures 16 and 17, respectively.

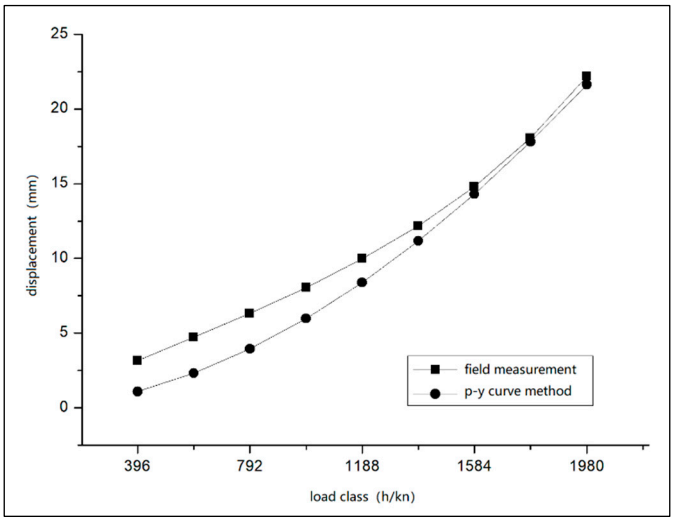


Figure 16. Comparison diagram of load–displacement curve of 2-8# test pile.

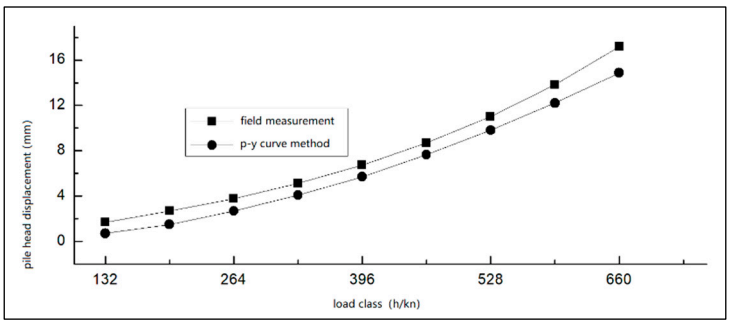


Figure 17. Comparison diagram of load–displacement curve of 2-X2# test pile.

From Figure 16, under a staged load, the maximum horizontal displacement calculated by the p-y curve method is approximately 21.63 mm and the maximum displacement

measured in field is 22.19 mm, a 0.56 mm difference. The calculated results are consistent with the measured trend, and the calculated results of horizontal bearing capacity of the single pile by the p-y curve method are close to the actual situation.

As can be seen from Figure 17, under subsection load, the maximum horizontal displacement calculated by the p-y curve method is approximately 14.90 mm, and the maximum displacement measured in the field is 17.18 mm, a 2.28 mm difference. The calculated results are consistent with the measured trend, and the calculated results of the horizontal displacement of the inclined single pile by the p-y curve method are close to the actual situation.

5.2. Comparison of Finite Element Results and Analytical Solutions

5.2.1. The P-Y Curve Pile Group Effect Coefficient Method

For the pile group p-y curve method, the authors of [33] proposed the pile group effect coefficient method to apply a correction coefficient to each pile in the pile group according to the different pile spacing and row number through a large number of centrifuge tests, and multiply each row of piles by the p multiplier in the p-y curve. This method can well describe the pile group effect. Reese et al. [34] summarized a large number of experiments and give the P-factor empirical formula:

$$P_m = \prod_{i=1}^{n} P_{im} \tag{7}$$

where P_m is the P factor of pile m, and P_{im} is the reduction coefficient of pile i to pile m.

When there are multiple horizontal piles under load in the direction of load action, different reduction coefficients are adopted between piles according to their relative positions. Generally, the former row of piles is only slightly affected by the latter row of piles [35]. The field test results summarized the statistical results of the reduction coefficients of the front and back rows of piles as follows:

$$\begin{cases} p_f = 0.7\left(\frac{s}{d}\right)^{0.26} & 1 \le \frac{s}{d} < 4 \\ p_f = 1 & \frac{s}{d} \ge 4 \end{cases} \tag{8}$$

$$\begin{cases} p_b = 0.48\left(\frac{s}{d}\right)^{0.38} & 1 \le \frac{s}{d} < 7 \\ p_b = 1 & \frac{s}{d} \ge 7 \end{cases} \tag{9}$$

where P_f is the reduction coefficient of the front pile, P_b is the reduction coefficient of the back pile, s is the pile spacing, and d is the pile diameter.

5.2.2. The Calculation Result of the P-Y Curve Method

According to the pile top load distribution and the P-factor correction coefficient of the pile group effect coefficient method, the displacement, shear force, and bending moment of each row of piles are shown in Figures 18–20, respectively.

As shown in Figure 18, the pile deflection curve calculated by the p-y curve method and the finite element method under the action of a distributed load is similar in form, and the p-y curve considering the pile–soil nonlinearity can well reflect the actual situation of pile displacement. The difference between the displacement at the top of the pile and that calculated by the finite element method is small; the error is only 2.6 mm. It can be concluded that the internal force distribution calculated by the p-y curve method and the finite element method are sufficiently accurate.

Figure 19 shows that, under the action of a distributed load, the maximum shear force of each pile is generated at the top of the pile. With the increase in depth, the shear force of the pile decreases to zero and generates negative shear force. However, due to the assumptions of the p-y curve method, the soil reaction at a certain depth is different from that of the finite element method, resulting in some differences in the value of pile shear.

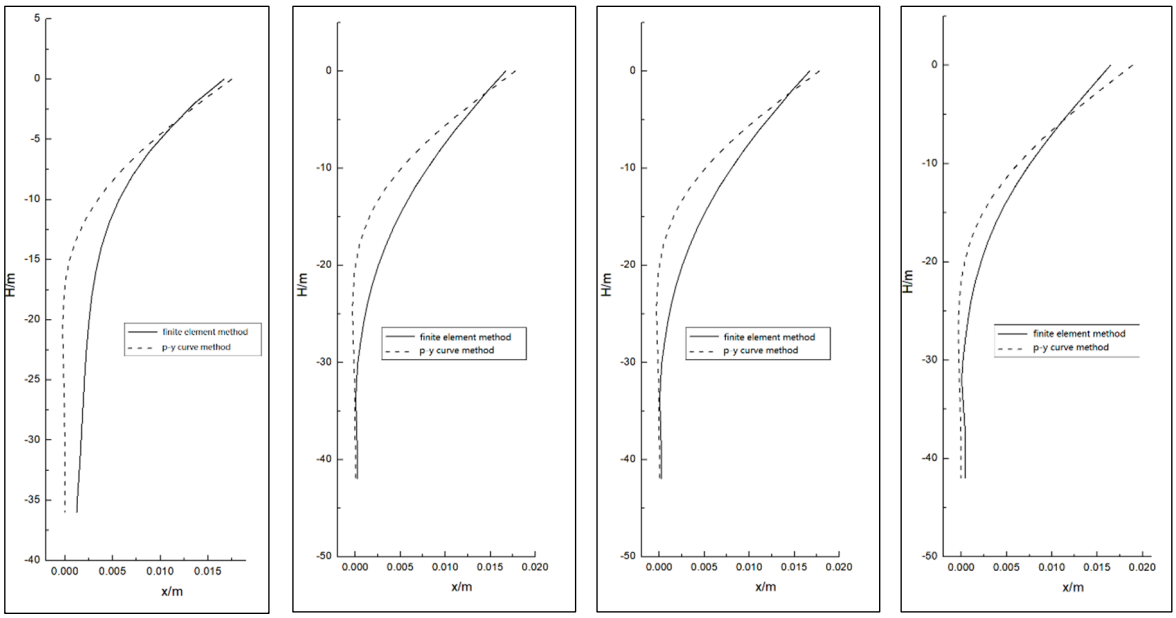


Figure 18. Pile displacement behavior: (**a**) inclined pile; (**b**) front pile; (**c**) middle row pile; (**d**) back pile.

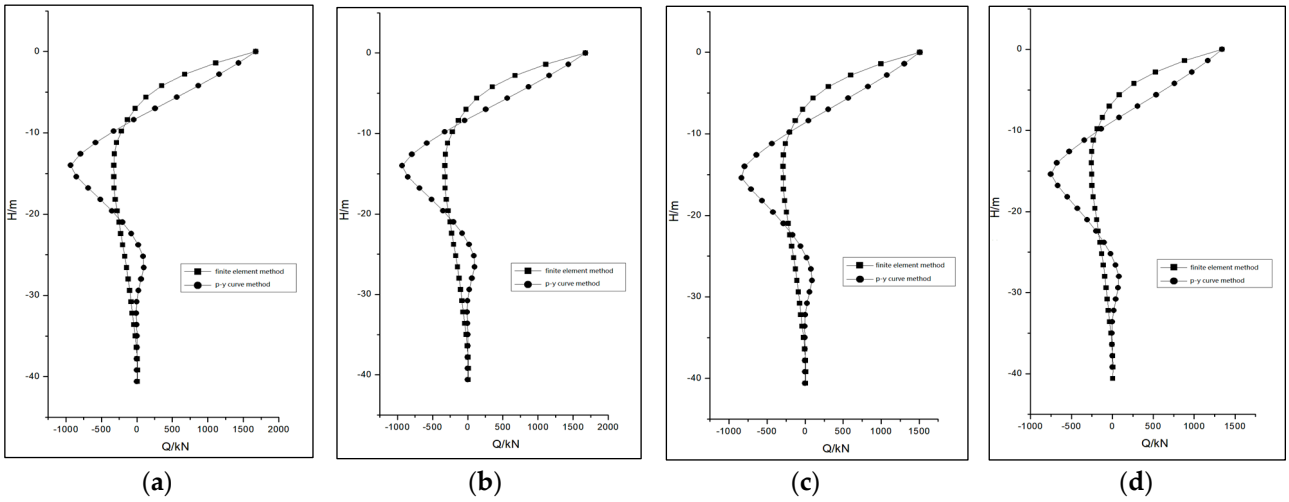


Figure 19. Pile shear force behavior: (**a**) inclined pile; (**b**) front pile; (**c**) middle pile; (**d**) back pile.

It can be seen from Figure 20 that the load was calculated to be properly distributed among the piles, and the pile bending moment calculated by the p-y curve method and the finite element method have similar variation trends. The inclined pile reaches the maximum bending moment at approximately 7 m and the straight pile reaches the maximum bending moment at approximately 9 m. As the negative shear calculated by the p-y curve method is large, the pile bending moment decreases more significantly below 10 m. Finally, the results of the p-y curve method are close to those of the finite element method only in a certain depth range.

Finally, according to the calculation theory of pile displacement and internal force, the shear strength and bulk density of the soil are also factors that affect the calculation results of the pile. When the shear strength and bulk density of the soil are higher, the displacement of the pile will be smaller. As a result, the strength of the soil mass can be increased by strengthening the foundation, improving the structure's safety. Therefore,

future research is needed to explore the influence of soil strength on the displacement and internal force of pile foundations.

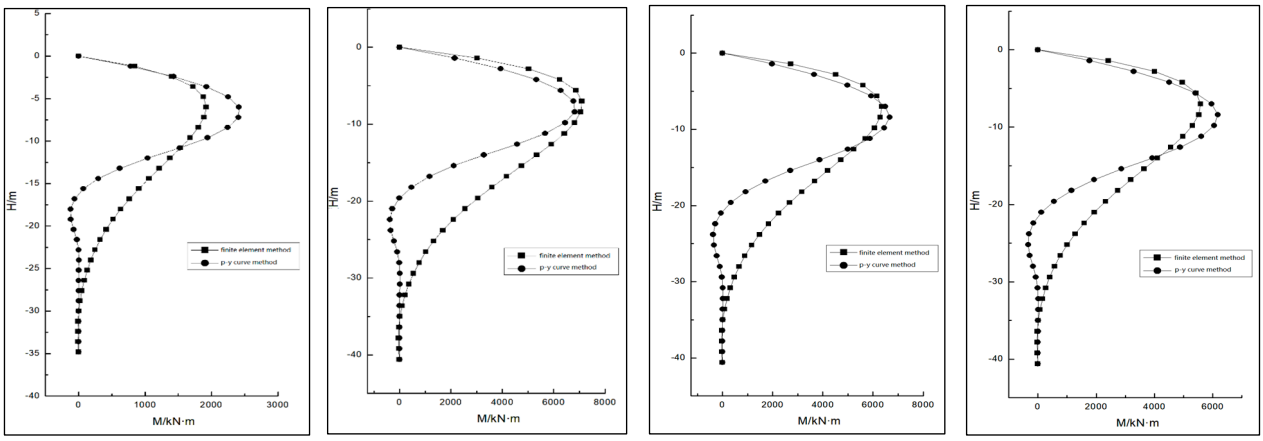


Figure 20. Pile bending moment behavior: (**a**) inclined pile; (**b**) front pile; (**c**) middle pile; (**d**) back pile.

6. Conclusions

According to the verified finite element model of the pile group, the displacement and internal force of each pile in the pile group of No. 2 cap under the action of basic combination after the bridge is completed were analyzed, and the p-y curve method was adopted to verify the load distribution. The following are the main conclusions:

1. The finite element method was used to calculate the force of the complex pile group foundation. The horizontal displacement behavior and internal force distribution of the pile group were analyzed under the basic load combination after the bridge was formed. The results show that the overall displacement trend of each pile is similar, and the pile top has a maximum displacement of approximately 16.7 mm.
2. The internal force analysis of 12 single piles on the No. 2 cap shows that the displacement shear of piles in different columns is slightly different under the influence of the edge effect. The pile in the second column suffers from the superposition of stress caused by the first and third columns, which makes the overall displacement of the pile in the second column generally greater than that of the first and third columns. Therefore, the shear of piles in the inner row is 2.5% larger than that of piles in the outer row. The stress of the middle and back piles overlaps as a result of the front pile's stress distribution. The forces of the inclined pile, the front pile, the middle row pile, and the back row pile are slightly different. For the same straight pile, the front row pile receives more load, while the middle row pile bears less load than the front row pile.
3. The maximum shear force of each pile body occurs at the top of the pile, and the maximum bending moment occurs at a point 1/5 away from the top of the pile. In the design of reinforcement, a stirrup at the top of the pile and a bending steel bar 1/5 away from the top of the pile can be added.
4. According to the bending moment and axial force calculated by the finite element method and the nonlinear calculation results of the p-y curve, the two methods are very close to each other in curve shape and value, indicating that the pile top load distribution is close to the actual situation. The p-y curve method is suitable for the calculation of bridge pile foundations. Finally, the displacement and internal force of piles under the influence of the pile group effect are studied as the soil depth changes. By comparing the p-y curve method with the finite element method, the calculation of the p-y curve method is reasonable to a certain extent. However, the parameters that affect pile calculation, such as the soil shear strength and the soil bulk density, are not analyzed. Consequently, the effects of the soil parameters on the displacement and

internal force of pile foundations using numerical modeling are the scope of interest for future research.

Author Contributions: Conceptualization, H.Q., H.W., M.A., Z.Z. and B.L.; formal analysis, M.A. and H.W.; investigation, H.Q., H.W. and M.A.; writing—original draft preparation, M.A., H.W. and H.Q.; supervision, H.Q. All authors have read and agreed to the published version of the manuscript.

Funding: The publishing of this paper is financially supported by the National Natural Science Foundation of China (No. 11672215).

Data Availability Statement: The data presented in this study are available on request from the corresponding author.

Conflicts of Interest: The authors declare no conflict of interest.

References

1. Qiu, H.; Zhou, Y.; Ayasrah, M. Impact Study of Deep Foundations Construction of Inclined and Straight Combined Support Piles on Adjacent Pile Foundations. *Appl. Sci.* **2023**, *13*, 1810. [CrossRef]
2. Anagnostopoulos, C.; Georgiadis, M. Interaction of vertical and lateral pile responses. *J. Geotech. Eng.* **1993**, *119*, 793–798. [CrossRef]
3. Karthigeyan, S.; Ramakrishna, V.V.G.S.T.; Rajagopal, K. Influence of vertical load on the lateral response of piles in sand. *Comput Geotech.* **2006**, *33*, 121–131. [CrossRef]
4. Meyerhof, G.G.; Yalcin, A.S. Behaviour of flexible batter piles under inclined loads in layered soil. *Can. Geotech. J.* **1993**, *30*, 247–256. [CrossRef]
5. Meyerhof, G.G.; Sastry, V.V.R.N.; Yalcin, A.S. Lateral resistance and deflection of flexible piles. *Can. Geotech. J.* **1988**, *25*, 511–522. [CrossRef]
6. Meyerhof, G.G. Behaviour of pile foundations under special loading conditions: 1994 RM Hardy keynote address. *Can. Geotech. J.* **1995**, *32*, 204–222. [CrossRef]
7. Chien, C.J.; Lin, S.S.; Yang, C.C.; Liao, J.C. Lateral performance of drilled shafts due to combined lateral and axial loading. *J. Mech.* **2013**, *29*, 685–693. [CrossRef]
8. Lee, J.; Prezzi, M.; Salgado, R. Influence of Axial Loads on the Lateral Capacity of Instrumented Steel Model Piles. *Int. J. Pavement Res. Technol.* **2013**, *6*, 80–85.
9. Mu, L.; Huang, M.; Lian, K. Analysis of pile-raft foundations under complex loads in layered soils. *Int. J. Numer. Anal. Methods Geomech.* **2014**, *38*, 256–280. [CrossRef]
10. Mahmood, M.R.; Salim, N.M.; Abood, M.H. The behavior of laterally loaded single pile model in unsaturated cohesionless soil. *IOP Conf. Ser. Mater. Sci. Eng.* **2018**, *454*, 012175. [CrossRef]
11. Zheng, Z.; Liu, C. Application of p-y Curve Method in Foundation Pit Envelope. *J. Yangtze River Sci. Res. Inst.* **2019**, *36*, 101–105.
12. Randolph, M.F. A theoretical Study of the Performance of Piles. Ph.D. Thesis, University of Cambridge, Cambridge, UK, 1978.
13. Reese, L.C.; Cox, W.R.; Koop, F.D. Analysis of Laterally Loaded Piles in Sand. In Proceedings of the 6th Offshore Technology Conference, Houston, TX, USA, 5 May 1974; pp. 473–483.
14. Long, J.H.; Vanneste, G. Effects of cyclic lateral loads on piles in sand. *J. Geotech. Eng.* **1994**, *120*, 225–244. [CrossRef]
15. Mu, L.; Kang, X.; Feng, K.; Huang, M.; Cao, J. Influence of vertical loads on lateral behaviour of monopiles in sand. *Eur. J. Environ. Civ.* **2018**, *22*, s286–s301. [CrossRef]
16. American Petroleum Institute. *Recommended Practice for Planning, Designing, and Constructing Fixed Offshore Platforms—Working Stress Design*; American Petroleum Institute: Washington, DC, USA, 2010.
17. Dash, S.R.; Rouholamin, M.; Lombardi, D.; Bhattacharya, S. A practical Method for Construction of p-y Curves for Liquefiable Soils. *Soil Dyn. Earthq. Eng.* **2017**, *97*, 478–481. [CrossRef]
18. Moayedi, H.; Nazir, R.; Gör, M.; Kassim, K.A.; Foong, L.K. A new real-time monitoring technique in calculation of the py curve of single thin steel piles considering the influence of driven energy and using strain gauge sensors. *Measurement* **2020**, *153*, 107365. [CrossRef]
19. Sun, W. A p-y model for predicting the lateral nonlinear interaction between pile and soil-rock mixture material based on discrete element modeling. *Simul. Model. Pract. Theory* **2020**, *100*, 102060. [CrossRef]
20. Daoliu, N. Calculation Method and Model Test of Internal Force of Slope Foundation Pile Based on p-y Curve Method. Ph.D. Thesis, Changsha University of Science and Technology, Changsha, China, 2017.
21. Nie, H.J. Research on Bearing Capacity and Calculation Method of Horizontal Load Bearing Pile Under Slope Condition. Ph.D. Thesis, Hunan University, Changsha, China, 2018.
22. Laibin, S. Research on Calculation and Analysis Method of Bridge Pile Group Foundation in Slope Section with Poor Stability. Ph.D. Thesis, Southwest Jiaotong University, Chengdu, China, 2019.
23. Jian, Z.; Yurun, L.; Zhixiao, Y.; Xian, R. Distribution law of pile bending moment of Straight inclined pile group cap under soil coupling based on Spectrum analysis. *J. Rock Mech.* **2020**, *39*, 1–16.

24. Cao, W.P.; Xia, B.; Ge, X. Formation and application of hyperbolic p-y curves for horizontally loaded single batter piles. *J. Zhejiang Univ. Sci (Eng. Sci.)* **2019**, *53*, 1946–1954.
25. *JGJ106 2014*; The Professional Standards of People's Republic of China. Technical Code for Testing of Building Foundation Piles, S. China Architecture and Building Press: Beijing, China, 2014.
26. *JGJ94-2008*; Ministry of Housing and Urban-Rural Development of the PRC. Technical Code for Building Pile Foundation. China Building Industry Press: Beijing, China, 2008.
27. Ayasrah, M.; Qiu, H.; Zhang, X.; Daddow, M. Prediction of Ground Settlement Induced by Slurry Shield Tunnelling in Granular Soils. *Civ. Eng. J.* **2020**, *6*, 2273–2289. [CrossRef]
28. Mengou, C.; Xiaoping, Y. Discussion on soil calculation range in finite element analysis of pile-raft foundation. *Guangdong J. Civ. Eng. Constr.* **2006**, *4*, 20–21.
29. Surarak, C.; Likitlersuang, S.; Wanatowski, D.; Balasubramaniam, A.; Oh, E.; Guan, H. Stiffness and strength parameters for hardening soil model of soft and stiff Bangkok clays. *Soils Found.* **2012**, *52*, 682–697. [CrossRef]
30. Ayasrah, M.; Qiu, H.; Zhang, X. Influence of Cairo Metro Tunnel Excavation on Pile Deep Foundation of the Adjacent Underground Structures: Numerical Study. *Symmetry* **2021**, *13*, 426. [CrossRef]
31. Qiu, H.; Wang, Z.; Ayasrah, M.M.; Fu, C.; Gang, L. Numerical study on the reinforcement measures of tunneling on adjacent piles. *Symmetry* **2022**, *14*, 288. [CrossRef]
32. Jacky, J. The coefficient of earth pressure at rest. *J. Soc. Hung. Archit. Eng.* **1994**, *7*, 355–358.
33. Brown, D.A.; Morrison, C.; Reese, L.C. Lateral load behavior of pile group in sand. *J. Geotech. Eng.* **1988**, *114*, 1261–1276. [CrossRef]
34. Reese, L.C.; Wang, S.T.; Arrellaga, J.A.; Hendrix, J. GROUP version 4.0 for Windows users' manual, Ensoft, Ine. Austin, Tex. 1996.
35. Jian, W.; Jianhua, W. Theoretical study on P-factor in pile group effect under horizontal load. *Chin. J. Geotech. Eng.* **2015**, *29*, 135–137+157.

Disclaimer/Publisher's Note: The statements, opinions and data contained in all publications are solely those of the individual author(s) and contributor(s) and not of MDPI and/or the editor(s). MDPI and/or the editor(s) disclaim responsibility for any injury to people or property resulting from any ideas, methods, instructions or products referred to in the content.